Plant Soil (2025) 513:333–351
https://doi.org/10.1007/s11104-024-07181-w

RESEARCH ARTICLE

Rooting for microbes: impact of root architecture on the microbial community and function in top- and subsoil

Adrian Lattacher · Samuel Le Gall · Youri Rothfuss · Chao Gao · Moritz Harings · Holger Pagel · Mona Giraud · Samir Alahmad · Lee T. Hickey · Ellen Kandeler · Christian Poll

Received: 7 June 2024 / Accepted: 19 December 2024 / Published online: 8 January 2025

Abstract

Background and aims Climate change and associated weather extremes pose major challenges to agricultural food production, necessitating the development of more resilient agricultural systems. Adapting cropping systems to cope with extreme environmental conditions is a critical challenge. This study investigates the influence of contrasting root system architectures on microbial communities and functions in top- and subsoil.

Methods A column experiment was performed to investigate the effects of different root architectures, specifically deep (DRS) and shallow (SRS) root systems of wheat (*Triticum aestivum* L.) on microbial biomass, major microbial groups, and extracellular enzyme activities in soil. We focused on β-glucosidase (BG) activity, which is an indicator for microbial activity, during different plant growth stages, using destructive and non-destructive approaches.

Results We found that the DRS promoted microbial biomass and enzyme activity in subsoil, while the SRS increased the microbial biomass and enzyme activity in topsoil. *In-situ* soil zymography provided fine-scale spatial insights, highlighting distinct patterns of BG activity near root centers and formation of enzyme activity hotspots, which were defined as regions where enzyme activity exceeds the mean activity level by 50%. Temporal changes in BG activity further underscored the dynamic nature of root-microbe interactions. Extracellular enzyme activities

Responsible Editor: Paul Bodelier.

Supplementary Information The online version contains supplementary material available at https://doi.org/10.1007/s11104-024-07181-w.

A. Lattacher (✉) · C. Gao · E. Kandeler · C. Poll
Soil Biology Department, Institute of Soil Science and Land Evaluation, University of Hohenheim, Emil-Wolf-Str. 27, 70599 Stuttgart, Germany
e-mail: adrian.lattacher@uni-hohenheim.de

S. Le Gall · Y. Rothfuss · M. Harings · M. Giraud
Institute of Bio- and Geosciences (IBG-3), Forschungszentrum Jülich GmbH, 52428 Jülich, Germany

H. Pagel
Soil Systems Modelling: Institute of Bio- and Geosciences (IBG-3), Forschungszentrum Jülich GmbH, 52428 Jülich, Germany

H. Pagel
Institute of Crop Science and Resource Conservation, University of Bonn, 53115 Bonn, Germany

S. Alahmad · L. T. Hickey
Queensland Alliance for Agriculture and Food Innovation, The University of Queensland, St Lucia, QLD 4072, Australia

indicated varying carbon, nitrogen and phosphorus acquisition strategies of rhizosphere microorganisms between top- and subsoil.

Conclusion This study underscores the need to consider root system architecture in agricultural strategies, as it plays a crucial role in influencing microbial communities and enzyme activities, ultimately affecting carbon and nutrient cycling processes in top- and subsoil.

Keywords Zymography · Rhizosphere · Enzyme distribution · Hotspots · Wheat

Introduction

Climate change and its associated weather extremes, such as less frequent but more intense rainfall, which leads to flooding and soil erosion, pose an increasing challenge for agricultural food production (Baveye et al. 2020; Habib-ur-Rahman et al. 2022). Therefore, the adaptation of crops to more extreme environmental conditions is necessary to create more resilient agroecosystems (Langridge et al. 2021). While the importance of above-ground plant biomass traits for the adaptation of crops to different environmental conditions is well understood, genotype selection increasingly considers the belowground plant traits related to root systems (Rambla et al. 2022; Voss-Fels et al. 2018). Current breeding approaches target the development of root ideotypes for more resource-efficient and stress-resistant crops (Paez-Garcia et al. 2015; Lynch 2019).

Root architecture largely determines the capability of plants to take up water and nutrients from different soil layers (Manschadi et al. 2006; Voss-Fels et al. 2018). Depending on the prevailing environmental conditions, different root architectures can be selected to increase yield (Rambla et al. 2022). Two of the most studied "root ideotypes" — an occasionally used term that corresponds to a combination of morphological and physiological root traits that are considered optimal for plant performance in a particular environment — are the so-called "steep, cheap and deep" and "topsoil foraging" types (Martre et al. 2015). While the former develops a rather deep root system due to a narrower root growth angle, the latter develops a somewhat shallow root system due to a wider root growth angle (Lynch 2022). These root systems offer various advantages and disadvantages in terms of nutrient and water uptake as well as construction and maintenance costs of the root systems themselves (Lynch 2013; Voss-Fels et al. 2018).

Roots alter the prevailing environmental conditions in soil by (1) increasing C inputs through rhizodeposition, (2) taking up water through the root system, leading to a decline in soil moisture, (3) changing the soil pH, and (4) creating macropores that can alter the oxygen content as well as water/nutrient infiltration due to improved diffusion pathways (Galindo-Castañeda et al. 2022). Deep and shallow root systems can therefore, by rooting through different soil layers with varying intensities, have distinct effects on the soil environment. These changes have a direct impact on resource quality and quantity and therefore on the composition and function of the soil microbial community. In particular, C input into the subsoil by deep root systems provides local soil microorganisms with an easily available energy source in an otherwise C poor habitat, which may result in a shift in microbial community structure as well as increased microbial biomass and nutrient turnover (Dennis et al. 2010; Galindo-Castañeda et al. 2023). While the benefits of different root architectures on the uptake of valuable soil resources such as nitrogen and water are well studied, less is known about their impact on the proliferation, composition, and function of soil microorganisms (Nakhforoosh et al. 2019; Paez-Garcia et al. 2015; Van der Bom et al. 2020).

A useful tool to detect changes in microbial functions is enzyme activity (Bauer et al. 1991; Dick and Kandeler 2005). Although plants and animals can also release enzymes, most enzymes in soil are of microbial origin (Alkorta et al. 2003; Dick and Kandeler 2005; Tabatabai 1994). In particular, hydrolases, such as β-glucosidase (BG), N-acetyl-β-glucosaminidase (NAG) and acid phosphatase (AP), which are closely related to the cycling of important elements in the soil such as C, N, and phosphorus (P), are important indicators of soil microbial functions and may reflect changing environmental conditions more rapidly than changes in the composition of the soil microbial community (Alkorta et al. 2003; Ferraz de Almeida et al. 2015; Makoi and Ndakidemi 2008). The enzyme profile of the rhizosphere is also known to be a footprint of plant-microbial interactions (Gianfreda 2015; Inamdar et al. 2022), since it depends on environmental changes

due to root growth and on the genetic potential of the soil microbial community to produce different enzymes. Whereas sampling of rhizosphere soil in the past did not permit elucidation of the spatial dimension of soil microbial processes in the rhizosphere, Spohn et al. (2013) were among the first to apply soil zymography to visualize the two-dimensional spatial distribution of relative enzyme activity *in-situ*. Subsequently, soil zymography has been further used to determine areas of high and low enzyme activity, further referred to as "hot- and coldspots", within the bulk soil, detritusphere, and rhizosphere (Bilyera et al. 2020; Ma et al. 2017, 2018; Spohn and Kuzyakov 2014). By linking enzyme activity with root system architecture, thus, one is better able to comprehend how different root structures shape microbial functions in both top- and subsoil.

The main objective of this study was to understand how differences in root system architecture caused by differences in seminal root angles affect the distribution of major microbial groups, microbial biomass, and microbial nutrient mobilization in top- and subsoil. Which with a few exceptions, has not been fully investigated in other studies (Galindo-Castañeda et al. 2023). For this, we selected two experimental spring wheat lines with strongly contrasting seminal root angles. A wide root angle usually favors the formation of a shallow root system (SRS), whereas a narrow root angle leads to the formation of a deep root system (DRS) (Kang et al. 2024). To explore the differences in microbial abundance and activity across the experimental period, we used two approaches: (1) soil zymography (*in-situ*) to determine the spatial distribution of the relative activity of BG, an indicator of microbial C cycling and thus important in the degradation of organic matter and the associated release of nutrients: and (2) destructive sampling of rhizosphere soil to provide sufficient amount of soil for analyses of microbial abundance and community structure. Both microbial biomass and enzyme activity in soils, especially in deeper soil layers, are largely dependent on C input by roots. Therefore, we hypothesized that 1) differences in quality and quantity of rhizodeposits of SRS and DRS will stimulate microbial biomass and modify community structure in top- and subsoil, respectively. We also hypothesized that 2) this will allow to link these differences to the spatial dimension of the rhizosphere of both genotypes.

Materials and methods

Experimental setup

The soil was collected in November 2020 from the upper 30 cm of a Haplic Luvisol (Cai et al. 2016) in an agricultural field located in Selhausen, Germany (50°52′07.8″ N, 6°26′59.7″ E), with a silt loam texture (22% clay, 66% silt, 12% sand) (Weihermüller et al. 2007). After sampling, the soil was homogenized, sieved to < 2 mm, and air-dried. The columns (8 cm inner diameter and 45 cm high) were filled with air-dried soil and compacted to reach a dry bulk density of 1.5 g cm^{-3}, representative of field conditions. The soil inside the columns was therefore compacted by carefully tapping the sides of the columns with a hammer to achieve a bulk density that is as homogenous as possible within the soil columns.

The two experimental spring wheat lines (*Triticum aestivum* L.) examined in this study were UQR012 (SRS) and UQR015 (DRS), which were developed by backcrossing a donor source for narrow root angle to the high-yielding spring wheat cultivar Borlaug100, as reported by Rambla et al. (2022). The genotypes UQR012 and UQR015 were selected because they displayed contrasting seminal root angles (RA°: 110° and 66°), which made them ideal for investigating the effect of root distribution on the composition and function of microbial communities at different soil depths. The genotypes were planted in monocultures; a total of four seeds were sown per column and after emergence the two strongest seedlings were retained. Plants were grown in a climate chamber under controlled conditions at light intensity of 1000 µM m^{-2} s^{-1} using a 12 h photoperiod (from 8 am to 8 pm). The temperature was set to 20 °C during the day and 18 °C at night, with humidity of 50%. The soil columns were saturated with deionized water by capillary action from the bottoms of the columns, which may have caused unintended clay dispersion in all treatments that was not accounted for in the experimental design. The mean initial soil volumetric water content (θ_{soil}) was 0.375 cm^3 cm^{-3}. During plant growth, water was added twice a week to keep the average θ_{soil} value across the columns between 0.225 cm^3 cm^{-3} and 0.405 cm^3 cm^{-3}. The required amount of water to maintain the soil moisture was calculated by the weight loss of the columns. A total of 13 columns per genotype were used (Fig. 1a), three

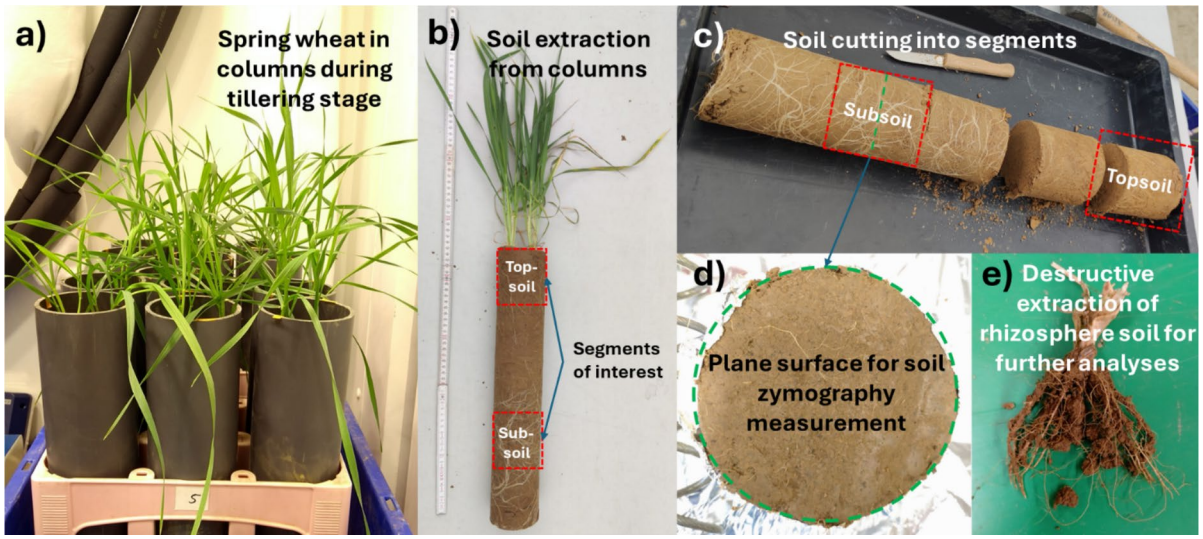

Fig. 1 Experimental setup and sampling procedure: **a**) the columns in the climate chamber, **b**) the soil extracted from the columns (here during tillering stage), **c**) soil cutting into segments of 9 cm, d) soil zymography (with soil segments 0–9 and 27–36 cm), and e) extraction of roots with adhering soil to obtain rhizosphere soil (after zymography)

of which were destructively sampled at 28, 35 and 42 days after sowing (DAS) and the remaining four 49 DAS, corresponding to the tillering, stem elongation, booting, and ear emergence stages, respectively (Fig. 1b). On each sampling day, aboveground plant biomass was removed and the soil was taken out of the columns and cut into horizontal segments of 9 cm thickness representing soil depths of 0 – 9 cm (further referred to as topsoil) and 27 to 36 cm (further referred to as subsoil) (Fig. 1c). The soil cores were stored at −20 °C till the zymography measurements. To obtain the plane surfaces required for soil zymography the 9 cm thick soil cores were cut in half using a sharp knife. After performing non-destructive analysis on the soil cores (zymography) (Fig. 1 d), the rhizosphere was sampled by removing all roots including the attached soil < 5 mm by hand (Fig. 1e) (Gobran and Clegg 1996). Rhizosphere soil was collected from the roots by gently shaking for 1 min in a plastic container. The rhizosphere soil was used for all further analyses and stored at −20 °C until analysis.

Soil zymography and image analysis

Soil zymography was performed on the plane surfaces (Fig. 1d) of the extracted top- and subsoil segments (Fig. 1c) according to Razavi et al. (2016). The fluorogenic substrate 4-methylumbelliferone-β-D-glucopyranoside (Sigma Aldrich, Germany) was used to determine the spatial distribution of the BG activity. The substrate was dissolved in dimethyl sulfoxide (Sigma Aldrich, Germany) and diluted to a concentration of 5 mM using deionized and autoclaved water. A polyamide membrane filter with of pore size 0.2 µm (Sartorius, India) was soaked with the substrate solution and placed directly on the soil surface. Before placing the filter on the soil surface, the soil was slightly moistened to allow sufficient diffusion of the substrate into the soil (Guber et al. 2021). The filter was incubated on the soil for 1 h in the dark at 20 °C. Afterwards the filter was removed and exposed to UV light (365 nm) using the BioDOC Analyzer (Biometra, Germany). The upper soil layer which was in contact with the substrate-soaked filter was removed after the measurement in order not to interfere with further measurements. Pictures were taken (RICOH TV-200 M 8–48 mm) with an exposure time of 75 ms and an enhancement of 5 using the BioDocAnalyze software. Small membrane snippets (3 × 1 cm) were soaked in solutions of increasing concentrations of 4-methylumbelliferone (MUF) (0, 0.05, 0.1, 0.15, 0.2 and 0.3 mM) for calibration. Enzyme activity was calculated by the volume of MUF solution, taken up by the polyamide membrane and its

size (Razavi et al. 2016). For both, the zymograms and the calibration, the same filters and camera settings were used.

We used the open-access software ImageJ (NIH, USA) with the package Fiji (Version 2.1.0) for image processing. The zymograms were converted into 8-bit grayscale images according to Bilyera et al. (2020) and the background fluorescence of filters soaked with MUF-substrate solution were subtracted from the gray values of the images. The loss of information by this conversion is considered uncritical as we were not interested in small-scale variations in enzyme activity within the range of the bulk soil. The gray values of the images were transformed into amount of MUF per membrane area (pM mm^{-2}) using the calibration function ($R^2 = 0.99$). A 1 × 1 cm piece of paper was used to set the scale using the "Set Scale" function of ImageJ. To compare the effect of the different root architectures on BG activity, average enzyme activity was calculated using the histogram data of the zymogram after calibration and background correction.

Enzyme activity hotspots were defined based on other studies that set the threshold for hotspots at > 50% above the mean enzyme activity. In this experiment, the threshold for hotspots corresponded to an enzyme activity of 11 pM mm^{-2} h^{-1} (Heitkötter and Marschner 2018; Hao et al. 2022). Accordingly, enzyme activity coldspots were defined as the areas that fell below 50% of the mean enzyme activity. The hot- and coldspot areas were calculated as percentages of the total soil surface area.

The BG activity gradient from the root center towards the surrounding soil was determined on selected roots with highest enzyme activity by using the "Plot Profile" function of ImageJ with a line width of five pixels (corresponding to 781 µm) on six to eight roots for each genotype, sampling time, and depth. The BG activity gradient was then plotted against the distance. The decrease in enzyme activity E(x) from the root center towards the surrounding soil was described using an exponential decay function:

$$E(x) = E_0 \cdot exp(-kx) + E_{bulk} \quad (1)$$

where E_0 is the initial enzyme activity (pM mm^{-2} h^{-1}) close to the root center, x is the distance to the root center (mm), k is a first-order rate coefficient (1/mm) of enzyme activity decrease and E_{bulk} represents the mean enzyme activity (pM mm^{-2} h^{-1}) in bulk soil. The exponential decay function was selected as a good approximation of the BG activity data, which showed an exponential decline with increasing distance from the roots down to the BG activity in the bulk soil (parameter E_{bulk}).

To determine the rhizosphere extent (R_{ext}), the rhizosphere threshold EΦ based on the BG activity in the bulk soil was calculated using the following equation:

$$E_\Phi = E_{bulk} + 2\sigma_{bulk} \quad (2)$$

where σ_{bulk} is the standard error of the mean enzyme activity (pM mm^{-2} h^{-1}) in bulk soil (E_{bulk}). This approach considers the natural variability in enzyme activity in the bulk soil by including two standard deviations, which statistically covers about 95% of the data. Consequently, this ensures that only areas with enzyme activity significantly higher than the bulk soil are defined as part of the rhizosphere.

E_{bulk} and σ_{bulk} were determined by measuring the BG activity of non-root affected areas in the zymogram. Areas with an enzyme activity equal to or greater than EΦ were considered as rhizosphere soil. To calculate the extent of the rhizosphere, Eq. 1 was modified by replacing E(x) with the rhizosphere threshold value EΦ, and the distance x was replaced by R_{ext}. This substitution allows for the determination of the distance R_{ext} from the root center at which the enzyme activity reaches EΦ. The extent of the rhizosphere (R_{ext}) in mm was therefore calculated using the following equation:

$$R_{ext} = -\ln\left(\frac{E_\Phi - E_{bulk}}{E_0}\right)/k \quad (3)$$

Potential enzyme activities in soil

The potential activity of three major enzymes involved in C-, N-, and P-cycling, i.e., BG (EC 3.2.1.21), NAG (EC 3.2.1.52) and AP (EC 3.1.3.2), were determined for rhizosphere soil according to Marx et al. (2001) by using fluorogenic 4-MUF substrates. Substrates and MES buffer were prepared according to Poll et al. (2006). To determine the enzyme activities, 1 g of rhizosphere soil was dispersed in 50 ml of deionized and autoclaved water by an ultrasonic disaggregator (50 J s^{-1}) for 2 min.

Afterwards, the suspensions were stirred on a magnetic stir plate and 50 µl aliquots were dispensed into 96-well microplates (PP F black 96 well, Greiner Bio-one GmbH, Germany). Subsequently, 50 µl of the autoclaved MES buffer and 100 µl of the substrate solution were added. For the standards, 50 µl of the soil suspension and an appropriate amount of standard solution and MES buffer were added to a final volume of 200 µl as reaction medium. The MUF concentrations of the standard solutions were 0, 100, 200, 500, 800, and 1200 pM per well. The plates were incubated under the exclusion of light at 30 °C. After a pre-incubation period of 30 min the fluorescence intensity at 460 nm was determined by exposing the plates to a wavelength of 360 nm using a microplate fluorescence reader (Bio-Tek Instruments Inc., FLX 800, Germany). Fluorescence was measured at 0, 30, 60, 120 and 180 min after the 30 min pre-incubation period. Enzyme activity (in $nM\ g^{-1}\ h^{-1}$) was determined using the linear correlation between the fluorescence intensity and the MUF concentrations of the standards.

Soil microbial carbon

Microbial carbon (C_{mic}) was determined using the chloroform fumigation extraction method by Vance et al. (1987). Two subsamples of 1 g rhizosphere soil were weighed from each sample. One subsample was fumigated in a desiccator with ethanol-free chloroform for 24 h to release C_{mic}. The remaining chloroform was then removed by flushing the desiccator 10 times with fresh air. Afterwards the fumigated and non-fumigated subsamples were extracted with 4 ml of 0.5 M K_2SO_4 solution, shaken at 200 U min^{-1} for 30 min, and centrifuged at 4400 g for 30 min. After shaking and centrifugation, the supernatant was transferred into a scintillation vial using a 5 ml pipette equipped with a 20 µm filter on the tip to avoid inclusion of organic particles. The extracts were frozen at −20 °C until measurement. Measurement of organic C in the supernatants was performed using the TOC-TNb Multi N/C 2100S Analyzer (Analytik Jena, Germany). Microbial biomass C was calculated by subtracting the C content of the non-fumigated from the fumigated extracts using the k_{EC} factor of 0.45 according to Joergensen (1996) to correct for the extractable part of total C bound to the microbial biomass. In addition, the non-fumigated samples were used to calculate the extractable organic C (EOC).

Phospholipid and neutral fatty acids

The main microbial groups were determined by extracting phospholipid and neutral fatty acids (PLFA, NLFA) from microbial cell membranes. The lipids were extracted from the rhizosphere soil, fractionated, and quantified according to Bardgett et al. (1996) based on the method of Frostegard et al. (1991) and Bligh and Dyer (1959). In brief, 4 g of soil was mixed with Bligh & Dyer solution (ratio of chloroform: methanol: citrate buffer = 1:2:0.8) to extract the lipids. To separate the NLFAs from PLFAs a solid phase extraction with extraction columns (Bond Elut, Agilent Technologies, USA) was used. Afterwards, the PLFAs and NLFAs were transformed into fatty acid methyl esters (FAMEs) by alkaline methanolysis, as described by Kramer et al. (2013). For quantification, an internal standard of the FAME C24:1 (Sigma-Aldrich, St. Louis, MO, USA) was added to the samples prior to methanolysis. Following Kandeler et al. (2015), the fatty acids i15:0, a15:0, i16:0, 16:1ω7, i17:0, cy17:0, and cy19:0 were chosen to represent bacterial PLFAs. The sum of iso and anteiso fatty acids was used as an indicator for the gram-positive bacteria ($PLFA_{Gram+}$) and the sum of cyclic fatty acids were used as an indicator for gram-negative bacteria ($PLFA_{Gram-}$). The fatty acid 18:2ω6,9 was chosen to represent fungi ($PLFA_{fun}$) (Federle 1986). Additionally, the NLFA 16:1ω5 was used as a biomarker for arbuscular mycorrhizal fungi ($NLFA_{AMF}$) (Olsson et al. 1998). The extracted FAMEs were analyzed on an Agilent 8860 gas chromatograph equipped with a 5977B mass selective detector (MSD) (Agilent, USA), calibrated with a bacterial methyl ester mix (Sigma-Aldrich, USA) and individual standard FAMEs.

Statistical analyses

Statistical analyses were conducted in R (Version 4.2.0) (R Core Team 2020). Normality and homogeneity of the enzyme activity, hotspot area of enzyme activity, rhizosphere extent, abundance of the main microbial groups and microbial carbon were analyzed using the Shapiro–Wilk´s test and Levene test from the car package for R (Fox and Weisberg 2019).

The significance of differences ($\alpha < 0.05$) of enzyme activity, hotspot area of enzyme activity, abundance of main microbial groups, and the microbial carbon were tested by a linear mixed-effects model using the lme function from the nlme package, where the columns were considered as a random effect and genotype, depth, and time as fixed effects (Pinheiro and Bates 2000).

To model the enzyme gradient within the rhizosphere a nonlinear mixed-effects model was fitted to the BG activity with increasing distance to the root center. This nonlinear mixed-effects model was simplified based on the significance of factors and interactions to identify the most important components of the model and to reduce overfitting. Significance of difference was then tested by performing an ANOVA on the simplified model.

To examine the relative focus of microbial acquisition on C versus nutrients (N and P) and P versus N acquisition, the untransformed proportional enzyme activity vector lengths (L_v) and angles (θ_v) were determined using the potential enzyme activity data of the BG, NAG and AP following the approach of Brandt et al. (2023) and Moorhead et al. (2016).

$$L_v = \sqrt{{E_{C-P}}^2 + {E_{C-N}}^2} \quad (4)$$

$$\theta_v = \mathrm{atan}(E_{C-P}, E_{C-N}) \quad (5)$$

In this context, $E_{C\text{-}P}$ indicates the relative activities of C- versus P-acquiring enzymes (BG/(BG + AP)), and $E_{C\text{-}N}$ represents the relative activities of C- versus N-acquiring enzymes (BG/(BG + NAG)). Using the arc tangent (atan), the vector angle of the line running from the origin of the diagram to the point ($E_{C\text{-}P}$, $E_{C\text{-}N}$) was calculated. Enzyme activity vectors thus reflect the relative resource requirements of the microbial community, independent of variations in total enzyme activity that may result from variations in total microbial biomass (Moorhead et al. 2016).

Results

Above- and belowground plant biomass

While neither the shoot- nor root biomass within top- and subsoil differed significantly within the different plant growth stages, mean plant biomass of the DRS across the different plant growth stages was significantly higher in shoot- and root biomass compared to the SRS (Figs. S1 and S2).

Microbial biomass and community structure in rhizosphere soil

In the topsoil, microbial biomass was similar between the two genotypes (Fig. 2). In the subsoil, microbial biomass of the DRS was higher than that of the SRS. Microbial biomass in the subsoil of the DRS increased from 113 to 159 µg C_{mic} g^{-1} between day 28 and 49, to levels comparable to the microbial biomass in topsoil of both the DRS (152 µg C_{mic} g^{-1}) and SRS (153 µg C_{mic} g^{-1}) at day 49**.**

The abundances of $PLFA_{Gram-}$, $PLFA_{Gram+}$, $PLFA_{fun}$ and $NLFA_{AMF}$ in rhizosphere were consistently higher in topsoil than in subsoil across all sampling dates (Fig. 3). In the topsoil, bacterial PLFAs ($PLFA_{Gram-}$ and $PLFA_{Gram+}$) had higher average abundance in the DRS compared to the SRS. Conversely, in the subsoil, they were higher in the SRS compared to the DRS. These differences

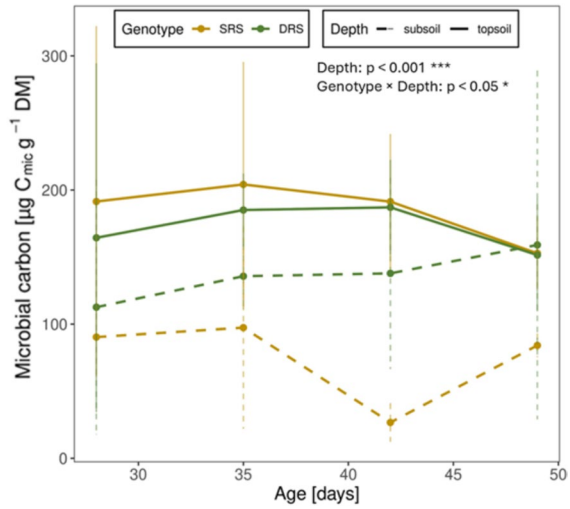

Fig. 2 Temporal changes in microbial carbon in topsoil and subsoil of the shallow root system (SRS) and deep root system (DRS) during the plant growth period. Points represent the mean of 3 replicates while the error bars represent standard deviation. The displayed p-values indicate significant effects ($p < 0.05$), determined using a linear mixed-effects model. In this model, the columns were treated as a random effect, while genotype, depth, and age were considered as fixed effects

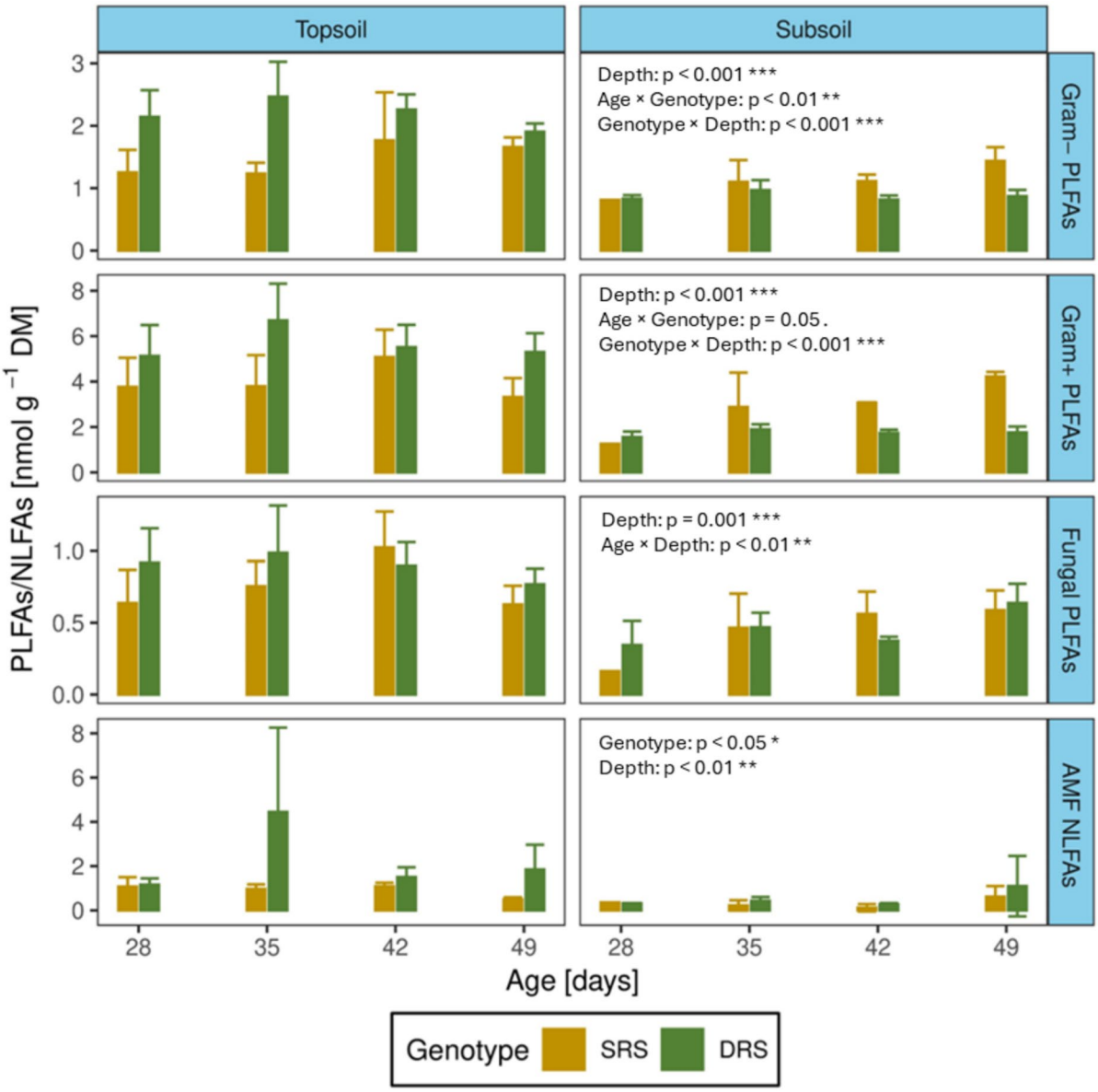

Fig. 3 Concentrations of phospholipid fatty acids (PLFAs) and neutral fatty acids (NLFAs) in n*M* g^{-1} DM of gram-positive (Gram+) and gram-negative (Gram-) bacterial PLFAs, fungal PLFAs, and arbuscular mycorrhizal (AMF) fungal NLFA in topsoil and subsoil of the shallow root system (SRS) and deep root system (DRS) from day 28 to day 49 after sowing. Error bars represent the standard deviation of three replicates. The displayed p-values indicate significant effects ($p < 0.05$), determined using a linear mixed-effects model. In this model, the columns were treated as a random effect, while genotype, depth, and age were considered as fixed effects. Due to the low rooting intensity of the SRS after 28 days in subsoil, it was not possible to extract enough rhizosphere soil in two out of three replicates. Therefore, no standard deviation can be shown for these samples

were observed for the interaction of genotype and soil depth. In contrast, the fungal PLFA and NLFA exhibited no statistically significant interaction effect of genotype and soil depth. The average fungal to bacterial (F:B) ratio across all sampling dates was higher for the SRS in top- than in subsoil and for the DRS in sub- than in topsoil (Fig. S3). Furthermore, the gram-positive to gram-negative

bacterial (GP:GN) ratio was higher for the SRS than DRS at both soil depths.

Extracellular enzyme activities in the rhizosphere

Except for the AP activity and the vector angle no significant differences in enzyme activities and stoichiometry were observed in the rhizosphere between the two genotypes. However, we found significant changes in enzyme activities over the experimental period between soil depths. Average BG and AP activities across all sampling dates were lower in subsoil than topsoil for both genotypes, while the NAG activity was similar between soil depths (Fig. S4). From 28 to 49 DAS, BG activity increased by 80% in the SRS topsoil, but stayed constant in the SRS subsoil and in both soil depths of the DRS. At the same time, NAG activity in the SRS increased by 50% in topsoil and 92% in subsoil. In contrast, NAG activity in the DRS decreased by 27% in the topsoil but increased by 26% in the subsoil.

To investigate the relative investment of rhizosphere microorganisms in C and nutrient (N and P) acquisition, the vector length and angle were calculated. During the experimental period, the vector length (Fig. 4a) increased in the topsoil and decreased in the subsoil of both genotypes (depth × age, $p < 0.05$). This result indicates that the relative investment of rhizosphere microorganisms into C as compared to nutrient acquiring enzymes increased in topsoil and decreased in subsoil over time. The vector angle (Fig. 4b) decreased in both soil depths of the SRS, hinting at an increasing relative focus on microbial N as compared to P acquisition over time, but was constant or even increased slightly in the DRS (genotype × age; $p < 0.01$).

Spatial distribution of β-glucosidase activity

The zymograms showed clear differences in BG activity between the DRS and SRS. Especially in subsoil, the DRS had higher BG activity than the SRS

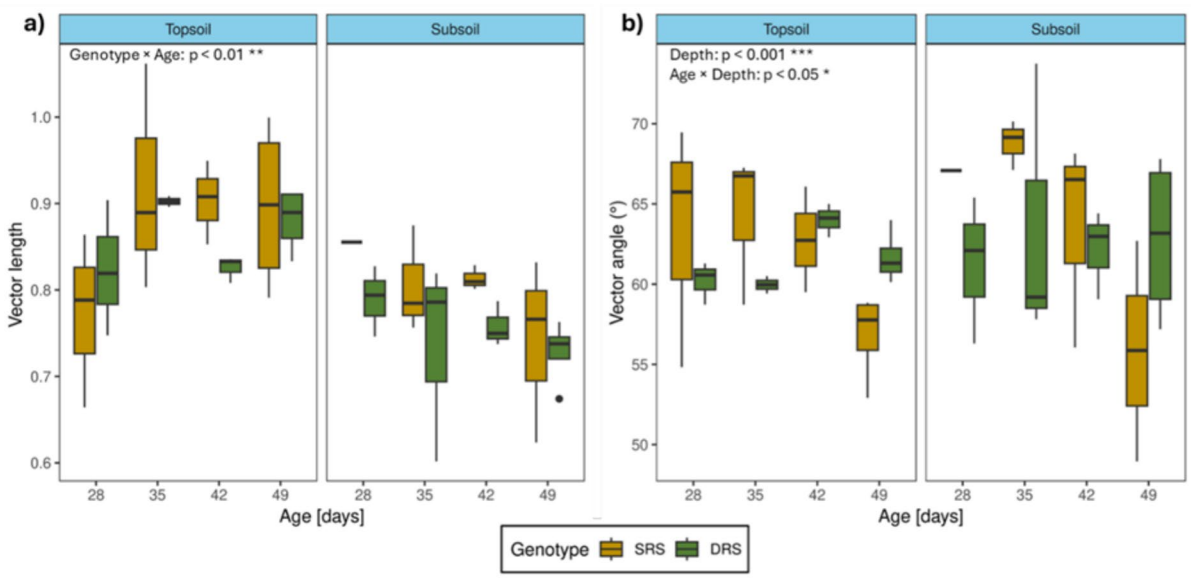

Fig. 4 Vector analysis of extracellular enzyme stoichiometry of BG to NAG (BG/(BG + NAG) versus BG to AP activity (BG/(BG + AP)) in topsoils and subsoils of the shallow root system (SRS) and deep root system (DRS). Boxplots are a) vector lengths and b) vector angles. The boxes in the boxplots represent the median and interquartile ranges. Whiskers extend to 1.5 times of the interquartile range. Points indicate outliers. The displayed p-values indicate significant effects ($p < 0.05$), determined using a linear mixed-effects model. In this model, the columns were treated as a random effect, while genotype, depth, and age were considered as fixed effects. Due to the low rooting intensity after 28 days in subsoil of the shallow root system (SRS), it was not possible to extract enough rhizosphere soil in 2 out of 3 replicates. Therefore, no standard deviation can be shown for these samples

(Fig. 5). The areas of highest enzyme activity (hotspots) were mainly located near the roots which were less visible in the subsoil of the SRS as compared to the DRS.

Depending on the prevailing root system type, temporal dynamics of the average BG activity was significantly different between top- and subsoil. In the SRS topsoil, there was a constant increase towards the highest mean BG activity 49 DAS with 12.5 pM mm^{-2} h^{-1} (+108%), whereas the DRS showed the same temporal pattern in the subsoil with the highest average enzyme activity of 8.78 pM mm^{-2} h^{-1} at the same sampling date (+165%, Fig. 6). Conversely, decreases of 32% and 19% in BG activity were observed in the SRS-subsoil and the DRS-topsoil, respectively. Averaged across all sampling dates, BG activity was higher in topsoil than subsoil in the SRS, while BG activity was similar between the soil depths in the DRS.

Enzyme activity hotspots and coldspots

The observed variations in average BG activity were also reflected in the enzyme activity hotspot areas. In the SRS-topsoil and the DRS-subsoil, hotspot areas increased from 28 to 49 DAS by 36% and 25%, respectively (Fig. 7). Conversely, a slight decrease in hotspot areas was observed in the SRS-subsoil and the DRS-topsoil (genotype × depth × age, $p < 0.05$). The BG coldspot areas in the SRS-topsoil and the DRS-subsoil decreased from 28 to 49 DAS by 32% and 30%, respectively. In contrast, the SRS-subsoil exhibited a strong increase in coldspot areas of 22%, while the coldspot areas in the DRS-topsoil decreased slightly from 28 to 49 DAS.

Dimension of the rhizosphere

BG activity was at its maximum directly at the root center and decreased exponentially with increasing distance from the root center to the surrounding soil after exceeding the rhizoplane (Fig. 8). In bulk soil, enzyme activity (E_{bulk}) was almost constant with increasing distance to the root center and was higher in topsoil compared to subsoil ($p < 0.05$). BG activity close to the root center (E_0) was influenced by the interaction effects of the genotypes and soil depth (genotype × depth, $p < 0.001$). In topsoil, BG activity

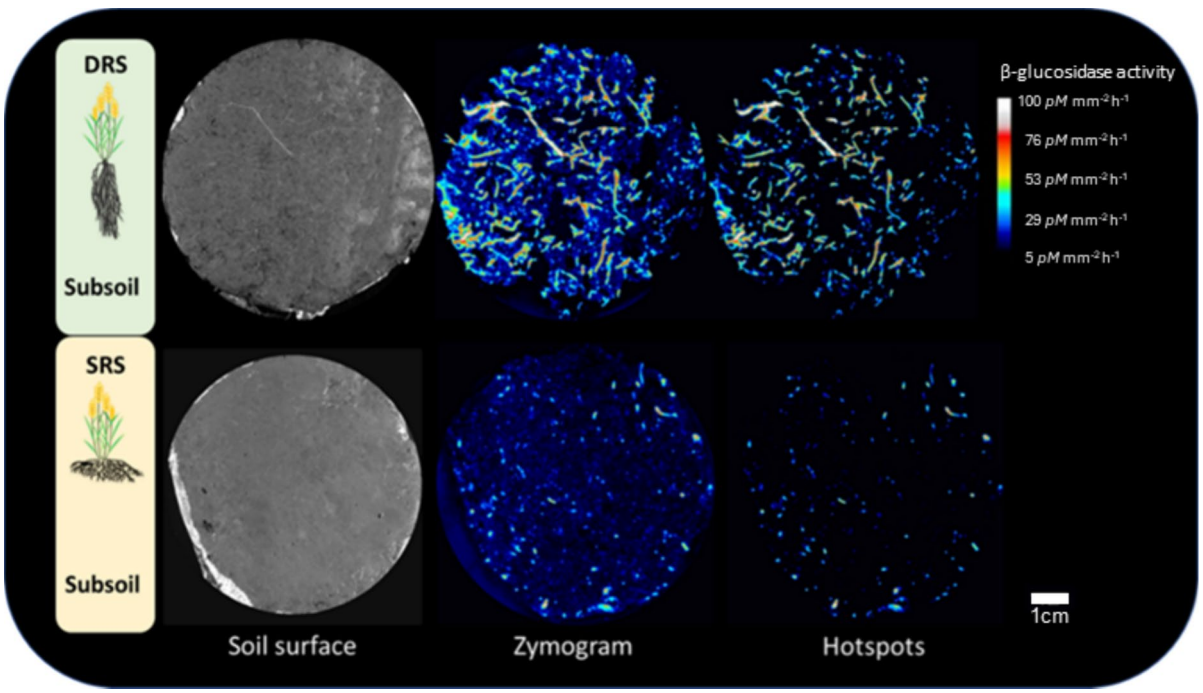

Fig. 5 Examples of images from the surface of the subsoil segment for both root systems (DRS and SRS) 49 days after sowing and the corresponding zymograms showing β-glucosidase activity and the associated hotspot areas

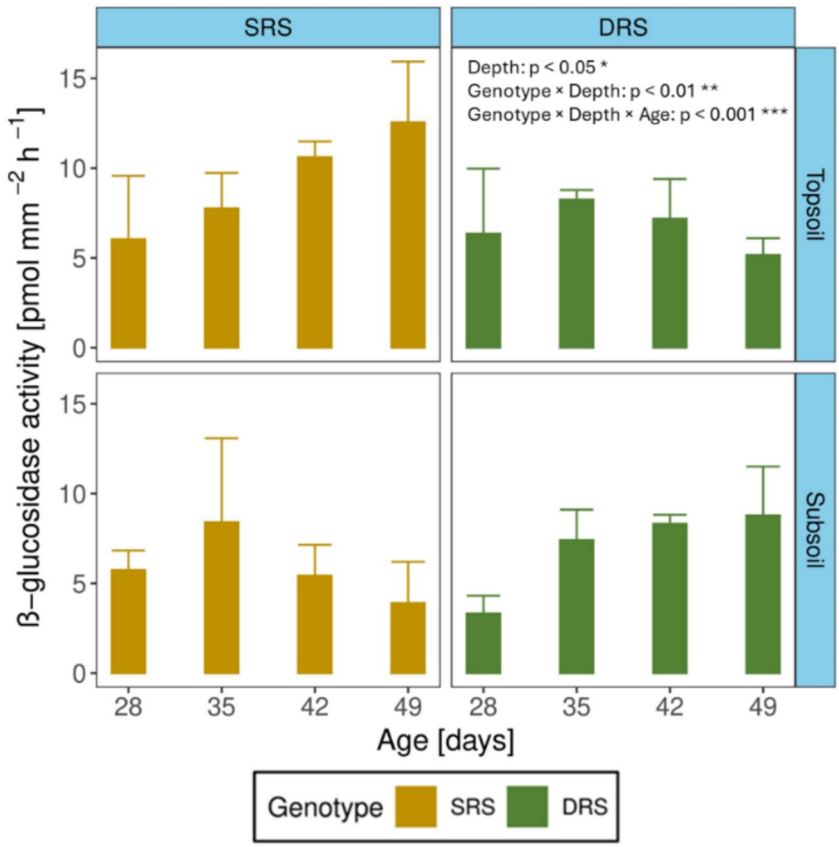

Fig. 6 Temporal patterns of the mean β-glucosidase activity in topsoil and subsoil for the shallow root system (SRS) (yellow) and deep root system (DRS) (green) from day 28 to day 49 after sowing. Error bars represent the standard deviation of 3 replicates. The displayed p-values indicate significant effects ($p < 0.05$), determined using a linear mixed-effects model. In this model, the columns were treated as a random effect, while genotype, depth, and age were considered as fixed effects

close to the root center was higher in the SRS than in the DRS and increased during plant growth (genotype × age, $p < 0.05$). In subsoil, the SRS had lower BG activity near the root center compared to topsoil and was also slightly lower than that of the DRS. The rate of decrease in BG activity (k) along the gradient was also different between genotypes ($p < 0.05$) and soil depths ($p = 0.053$). The rhizosphere extent (R_{ext}) of BG ranged from 0.71 to 1.36 mm from the root center, but was not significantly different among genotypes, soil depths, or plant age ($p = 0.864$).

Discussion

Our study investigated the effects of contrasting root system architectures (deep and shallow) of wheat on the microbial community and its function in top- and subsoil during a 7-week plant growth period. The average above- and below-ground plant biomass across all sampling dates in top- and subsoil of the DRS was higher compared to the SRS, indicating improved performance of the DRS under the prevailing conditions. Destructive (multi-substrate assay) and non-destructive *in-situ* (soil zymography) approaches were used to determine differences in microbial functions. We found that the DRS increased microbial biomass and BG activity in subsoil compared to the SRS over the growing period. Soil zymography showed that the different genotypes mainly affected the spatial distribution of BG activity, but not the absolute enzyme activity in the bulk rhizosphere soil.

Effect of the root system on microbial abundance and community structure

Our results demonstrate the impact of the root architecture on microbial abundance, especially in the subsoil. Microbial biomass of both genotypes was initially higher in topsoil than in subsoil. Its proximity to the soil surface may have resulted in a higher input of plant derived C and oxygen availability, in contrast to the subsoil, where resource availability

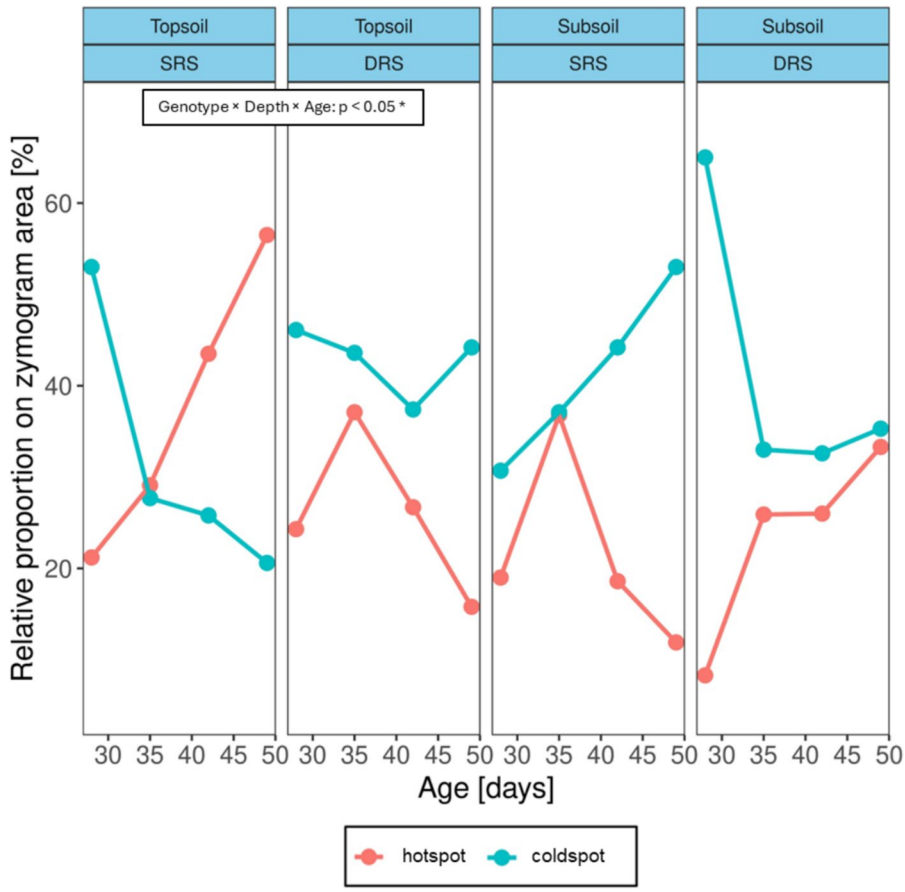

Fig. 7 Proportion of the β-glucosidase hot- and coldspots on the total zymogram areas for the shallow (SRS) and deep root system (DRS) in top- and subsoil from day 28 to day 49 after sowing. The displayed p-values indicate significant effects ($p < 0.05$), determined using a linear mixed-effects model. In this model, the columns were treated as a random effect, while genotype, depth, and age were considered as fixed effects

is lower (Beule et al. 2022). Towards the end of the experimental period, microbial biomass in the subsoil of the DRS reached levels comparable to the topsoil, indicating substantial microbial growth in response to increased rhizodeposits and substrate availability (Venzke Filho et al. 2004). Thus, deep root systems are an important source for soil microorganisms in the subsoil, where the input of fresh C and energy sources is scarce. This increase in microbial biomass in the subsoil can promote the mineralization of various nutrients (N, P and S) from different organic sources and enable microbes to convert organic matter into plant-available nutrients, promoting plant growth (Jacoby et al. 2017).

Despite lower root biomass in the subsoil of SRS than DRS (Fig. S1) PLFA patterns suggested greater abundance of bacteria, in particular of gram-positive bacteria, in the subsoil of SRS. These results contrasted with C_{mic} results, which suggested the opposite trend. The inconsistency between mainly cytoplasm C (measured by chloroform-fumigation extraction) (Högberg et al. 2007; Leckie et al. 2004) and PLFA contents (microbial cell membranes) could indicate a potentially less active/more dormant and less C-supplied microbial community in the SRS-subsoil than the DRS-subsoil (Joergensen and Wichern 2018). This indicates a distinct microbial response to the rhizodeposits and nutrient gradients in the subsoil, possibly driven by the specific architectural characteristics of the SRS. This is supported by the observed changes in the GP:GN ratio across the soil profile of the SRS. The topsoil of the SRS displayed a shift towards gram-negative bacteria over the experimental period, probably due to increasing availability of C-rich substrates in the rhizosphere. Gram-negative bacteria are known to utilize labile organic C compounds and often predominate within the rhizosphere (Fierer et al. 2003; Kennedy and de Luna 2005). In contrast, the significant increase in relative gram-positive bacterial abundance in the subsoil of

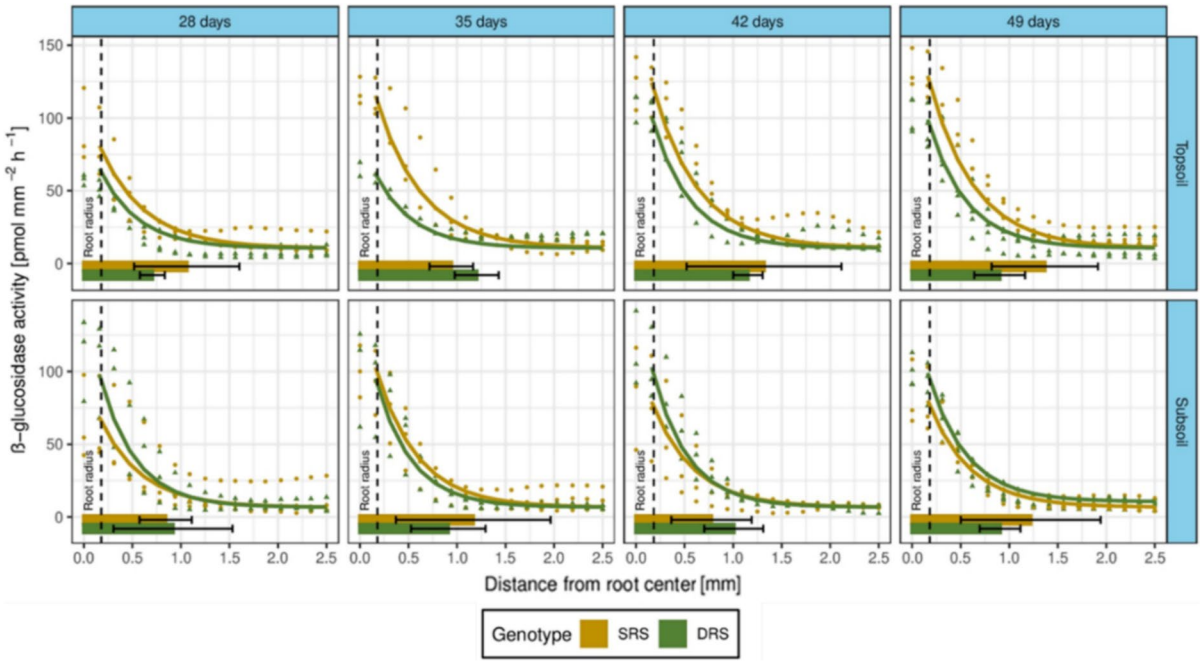

Fig. 8 Profile of the β-glucosidase gradient within the rhizosphere towards the surrounding soil for both the shallow root system (SRS) and deep root system (DRS). Dots represent the mean BG activity for the SRS (yellow dots) and DRS (green dots) per segment. Lines represent the fit of an exponential decay function to mean enzyme activity profiles estimated from image analysis of zymograms. The vertical dotted line represents average root radius. The horizontal bars show the rhizosphere extent of the SRS and DRS

the SRS and its absence in the DRS can be attributed to its lower root biomass and rhizodeposition. Gram-positive bacteria, known for their adaptation to more nutrient-limited conditions, may have responded to the evolving rhizodeposits in the subsoil as the plants matured (Kramer and Gleixner 2008; Wang et al. 2014). But the overall low level of rhizodeposits from low root biomass may not have been sufficient to support gram-negative bacteria.

In contrast to bacteria, fungal abundance was generally unaffected by the different root system architectures. However, a higher F:B ratio in the subsoil of the DRS compared to the SRS indicates a shift in nutrient availability within the rhizosphere, attributable mainly to the lower abundance of gram-positive bacteria in the DRS, particularly in comparison to the significantly higher abundance of gram-positive bacteria observed in the subsoil of the SRS. This transition in microbial composition could have been influenced by the different C utilization strategies of bacteria, which primarily utilize dissolved organic C, and fungi, able to utilize also more complex carbon sources such as cellulose and lignin (Eichlerová et al. 2015). In summary, the root system architecture plays a central role in the proliferation and composition of soil microorganisms at different soil depths in the rhizosphere, potentially affecting nutrient cycling and plant–microbe interactions.

Extracellular enzyme activity in rhizosphere soil

The classical approach to study the microbial biomass and enzyme activity in the rhizosphere is to destructively sample rhizosphere soil. The exact protocol for sampling rhizosphere soil is not uniformly defined in the literature and there are several approaches described (Angle et al. 1996; Barillot et al. 2013; Han et al. 2009; Mijangos et al. 2009; Smalla et al. 2001). Most of these approaches define the soil adhering to the roots as rhizosphere soil, which is generally removed from the roots either by shaking or washing. However, the amount of soil adhering to the roots is strongly influenced by the plant, the soil type (e.g. clay or sandy soils), and the water

content and, therefore, does not necessarily reflect the total or exclusive area influenced by roots (Barillot et al. 2013). Despite the limitations of the classical approach, it remains the only method for obtaining samples to analyze rhizosphere soil. The observed temporal variations in BG, AP, and NAG activities revealed the dynamic nature of C and nutrient cycling in the different root systems. The rise in BG activity in the topsoil of the SRS during the later stages of plant growth indicated a microbial response to changing rhizodeposits. Greater availability of cellulose-rich substrates such as root cell debris originating from the root border cells or border-like cells as the plants matured, potentially stimulated microbial cellulose degradation and growth (Driouich et al. 2013; Ropitaux et al. 2019). This is also in accord with the observed increase in the relative abundance of gram-negative bacteria in the SRS topsoil. Lower BG activity in the SRS subsoil than topsoil suggests that the quantity of rhizodeposits, influenced by lower rooting intensity, may not have been sufficient to promote the relative abundance of gram-negative bacteria. Interestingly, NAG activity remained stable across the root system architectures and soil depths, potentially related to the constant turnover of chitin-rich fungal cell walls in the rhizosphere and the subsequent release of N (Maillard et al. 2018). Based on the stable abundance of fungal PLFAs and activity of NAG, which is mainly produced by fungi by breaking and rebuilding their cell walls as they grow (Konkol et al. 2012), the different root systems seemed to have no significant impact on fungal growth and activity.

Although there was no great temporal variation in microbial biomass, in the topsoil of the SRS there was an increase in specific BG (+101%) and NAG (+106%) activities between 28 and 49 DAS. This suggests an increasing substrate concentration during progression of plant growth in the SRS topsoil and hence, a build-up of the extracellular enzyme pool, contributing to nutrient mineralization from soil organic matter (SOM) degradation. The calculated vector lengths and angles provided insights into the relative investment of rhizosphere microorganisms in C, N and P acquisition (Brandt et al. 2023; Moorhead et al. 2013). In the topsoil of both root systems, the increase in vector length over time indicated an increasing focus on the decomposition of organic matter for C acquisition. In contrast, in the subsoil, the decrease in vector length of both root systems indicated increasing relative nutrient (N and P) acquisition by the rhizosphere microbial community over time. The increasing focus on C as compared to nutrient acquisition in the topsoil indicates competition between microorganisms in the rhizosphere and plants for root nutrients, which could be further fueled by decreasing concentrations of SOC and DOC (Ai et al. 2012; Bi et al. 2022). Based on changes in enzyme stoichiometry, rhizosphere communities in the SRS and DRS appeared to reflect the dynamic adaptation strategies with which the microbial community reacted to changing nutrient availability at different soil depths during plant growth. The changes in vector angles indicated greater relative N acquisition in the SRS rhizosphere and increased relative P acquisition in the DRS rhizosphere. This highlights the nuanced responses of the microbial community to different root architectures and nutrient availability. Since nitrate is very mobile in soil and could therefore leach into the subsoil where the uptake by the SRS is limited due to the low root biomass, competition for N between SRS plants and rhizosphere microorganisms might have been higher compared to the DRS, which was able to obtain a large proportion of its nutrients from the subsoil. As P is relatively immobile in the soil, the input of P is mainly limited to the topsoil (Lynch 2011). This could have led to lower P uptake by DRS compared to SRS over time, in turn affecting the strategy of the root system from root exudation to mycorrhization (Ravi and Muthukumar 2024). The increased investment in P acquisition in the rhizosphere of DRS compared to SRS could, furthermore, be attributable to the DRS plant's higher AP production in response to its higher above- and belowground biomass. Moreover, higher AP production may also be mediated by the higher abundance of AMF in the DRS rhizosphere. In addition to increased water uptake by the plant, the higher abundance of AMF in the DRS topsoil than in the subsoil could lead to a greater secretion of P acquiring enzymes into the soil (Liu et al. 2018; Steidinger et al. 2015). Arbuscular mycorrhizal fungi can thus serve an important role in nutrient mobilization and enhancement of P availability and acquisition within the rhizosphere of the DRS. Overall, resource acquisition in the rhizosphere reflected microbial community structure, with an enrichment in gram-negative bacteria being linked to higher activity of BG. Vector analysis showed that the nutrient acquisition

strategies of rhizosphere microorganisms are affected by the mobility of nutrients in soil (mobile vs. immobile) and the ability of the different root systems to acquire them.

Impact of root systems on enzyme activity dynamics

While sampling of rhizosphere soil makes it possible to characterize microbial processes averaged across the entire rhizosphere, it falls short compared to enzyme zymography in providing reliable estimates for rhizosphere dimensions, spatial variations in enzyme activity and hotspot areas (Ma et al. 2018). The zymography measurements revealed distinct patterns in BG activity between the SRS and DRS: BG activity averaged across rhizosphere and bulk soil was higher in the subsoil of the DRS compared to the SRS and lower in the topsoil (Fig. 6). In principle, there are two potential explanations for this observation.

First, the observed differences in BG activity of SRS and DRS between topsoil and subsoil can be a result of differences in rooting intensity. Previous studies, which used in situ soil zymography, observed a strong link between the spatial distribution of hotspots and the distribution of roots (Hao et al. 2022; Kuzyakov and Blagodatskaya 2015; Sanaullah et al. 2016). Accordingly, the observed differences in average BG activity in our study corresponded to changes in the enzyme activity hotspots across the different soil layers; i.e., we found larger hotspot areas in the SRS-topsoil and DRS-subsoil compared to smaller hotspot areas in the SRS-subsoil and DRS-topsoil. We concluded, therefore, that the observed patterns in hot spot areas resulted in an increase in BG activity in the topsoil of SRS and in the more intensively rooted subsoil of DRS during plant growth. This inverse pattern was not observed in the classical approach, in which only the soil of the rhizosphere cylinder was sampled, and did not consider the differences in rooting intensity in the topsoil and subsoil between the two root systems. BG activity and hotspot areas in the topsoil of the DRS were lower than in the SRS, but DRS had a higher root biomass than the SRS. This apparent discrepancy may have been due to reduced release of root exudates by the DRS in topsoil resulting from differences in root age and root tissue type (primary root, lateral root, and root tip) between the two root systems (Sasse et al. 2018; Ulrich et al. 2022). As the formation of hotspots is an efficient strategy for plants to take up nutrients from the soil (Kuzyakov and Xu 2013), our observed temporal changes in the spatial distribution indicates the rhizosphere areas from which the SRS and DRS obtained most of their nutrients. In these areas, higher inputs of C and energy sources by the plant might have stimulated a priming effect that promoted the degradation of SOM and thus also the mineralization of important plant nutrients by soil microorganisms (Chen et al. 2019; Shang et al. 2023). The proportions of hotspot areas changed over the course of this experiment; this may be attributed to changes in the amount or composition of root exudates during plant growth. This accords with Iannucci et al. (2021), who showed that the quality and quantity of root exudates varies not only during the different phases of plant growth, but also between different genotypes of wheat with different root morphologies.

Second, not only the proportion of hotspot areas but also the spatial extent and the level of BG activity within each hotspot may explain the observed overall pattern in BG activity. In our study, the rhizosphere extent of BG ranged from 0.7 to 1.4 mm but was not significantly different between the genotypes and soil depths. The rhizosphere extent is known to be enzyme and plant-specific (Ma et al. 2018). Plants with thicker roots such as maize tend to form an up to 1.4 times greater rhizosphere than wheat (Ma et al. 2018). The BG gradient that had its maximum activity directly at the root center and decreased exponentially after passing the root surface showed distinct differences between top- and subsoil. The observed differences in BG activity near the root centers between genotypes and soil depths could be an indication of different nutrient uptake and release strategies (conservative and explorative/competitive) by the two root systems (Iannucci et al. 2021). Notably, the SRS seemed to focus its activity on the topsoil, while the DRS concentrated its activity more on the subsoil, which corresponds with the observed hotspot areas. For instance, the DRS may exhibit higher BG activity close to the root center in the subsoil, potentially due to differences in root age and root tissue type compared to the SRS, facilitating greater exudate release. Thereby, the proliferation of fast-growing microorganisms was stimulated, as reflected in the increase in microbial biomass in the subsoil of the DRS (Adetunji et al. 2017; Blagodatskaya et al. 2009; Kuzyakov and Xu 2013; Steinauer et al. 2016; Ulrich

et al. 2022). Although there may have been variations in enzyme activity close to the roots among the genotypes in the topsoil and subsoil, this did not result in a greater extent of the rhizosphere. Instead, it seems to have impacted microbial biomass C within the rhizosphere, which in turn affected the processes of nutrient turnover affecting plant performance.

Conclusion

One of our key findings was that root system architecture strongly affects microbial biomass and enzyme activity in different soil layers. Specifically, deep root systems were able to increase microbial abundance and enzyme activity in the subsoil to levels comparable to the topsoil of a shallow root system. The utilization of different sampling approaches, destructive and *in-situ*, highlighted the importance of methodological choices in interpreting enzyme activity within the rhizosphere. Considering the detailed spatial insights provided by non-destructive BG gradient analysis using soil zymography, this approach could offer a more nuanced understanding of enzyme dynamics within the rhizosphere, and beyond, compared to the broader, destructive multi-substrate assay. Soil zymography enabled us to capture fine-scale variations between genotypes of the same crop and to improve our ability to identify the intricate interactions between root system architecture and microbial processes in the rhizosphere. The zymography results showed not only the effect of the number of roots on enzyme activity, but also differences in enzyme activity within the rhizosphere between both root systems, with higher BG activity in SRS-topsoil and DRS-subsoil. The complex interactions between root architecture and microbial communities was further seen in the differing abundances of microbial groups as a possible response to root exudates and nutrient gradients. Our insights contribute to a deeper understanding of the complex interactions occurring within the rhizosphere, providing a foundation for future research aimed at optimizing plant–microbe interactions for enhanced agricultural productivity and resilience. While our study provided valuable information about the effect of root architecture of wheat genotypes on root-microbial interactions, it was restricted to the initial phase of plant growth due to limited space in the soil columns; future investigations, therefore, could explore the combination of wheat phenotypes with contrasting root system architectures within a single field to evaluate the effects of the observed rhizosphere processes on plant growth and yield.

Acknowledgements The authors thank Dagmar van Dusschoten, Sandisiwe Moyo, Christoph Tempelmann and Esther Vogt for their technical assistance during this work and Kathleen Regan for English corrections.

Authors' contributions Adrian Lattacher, Samuel Le Gall, Youri Rothfuss, Moritz Harings, Mona Giraud, Ellen Kandeler and Christian Poll contributed to the conception and design of the study. Samir Alahmad and Lee Hickey developed and provided the required wheat lines. Samuel Le Gall, Moritz Harings and Mona Giraud conducted the column experiment in the climate chamber. Adrian Lattacher and Chao Gao performed the sample analysis. Samuel Le Gall provided data on the shoot dry biomass. Adrian Lattacher conducted the data evaluation and statistics with contribution of Holger Pagel and Christian Poll. The first draft of the manuscript was written by Adrian Lattacher under supervision of Ellen Kandeler and Christian Poll. All authors commented on previous versions of the manuscript. All authors read and approved the final manuscript.

Funding Open Access funding enabled and organized by Projekt DEAL. This paper was written within the context of the phase I of the CROP project (Combining ROot contrasted Phenotypes for more resilient agro-ecosystem) (project number: FKZ 031B0909A), which is founded by the German Federal Ministry of Education and Research (BMBF). The experimental wheat lines examined in this study were developed through the Grains Research and Development Corporation (GRDC) "Rooty" project (ID 9176855), which formed part of the International Wheat Yield Partnership Consortium (IWYP122). Holger Pagel received additional funding from the Deutsche Forschungsgemeinschaft (DFG, German Research Foundation) under Germany's Excellence Strategy – EXC 2070–390732324.

Data availability The datasets generated during the current study are available at the BonaRes repository, https://doi.org/10.20387/bonares-80c6-ppnj

Code availability This is not applicable to the manuscript.

Declarations

Conflicts of interest The authors have no relevant financial or non-financial interests to disclose.

References

Adetunji AT, Lewu FB, Mulidzi R, Ncube B (2017) The biological activities of β-glucosidase, phosphatase and urease as soil quality indicators: A review. J Soil Sci Plant Nutr 17(3):794–807

Ai C, Liang G, Sun J, Wang X, Zhou W (2012) Responses of extracellular enzyme activities and microbial community in both the rhizosphere and bulk soil to long-term fertilization practices in a fluvo-aquic soil. Geoderma 173–174:330–338

Alkorta I, Aizpurua A, Riga P, Albizu I, Amézaga I, Garbisu C (2003) Soil enzyme activities as biological indicators of soil health. Rev Environ Health 18:65–73

Angle JS, Gagliardi JV, McIntosh MS, Levin MA (1996) Enumeration and expression of bacterial counts in the rhizosphere. Soil Biochemistry 9:233–251

Bardgett RD, Hobbs PJ, Frostegård Å (1996) Changes in soil fungal:bacterial biomass ratios following reductions in the intensity of management of an upland grass-land. Biol Fertil Soils 22:261–264

Barillot CDC, Sarde CO, Bert V, Tarnaud E, Cochet N (2013) A standardized method for the sampling of rhizosphere and rhizoplan soil bacteria associated to a herbaceous root system. Annals of Microbiology 63:471–476

Bauer E, Pennerstorfer C, Holubar P, Pias C, Braun R (1991) Microbial activity measurement in soil —a comparison of methods. J Microbiol Methods 14:109–117

Baveye PC, Schnee LS, Boivin P, Laba M, Radulovich R (2020) Soil organic matter research and climate change: Merely re-storing carbon versus restoring soil functions. Front Environ Sci 8:579904

Beule L, Guerra V, Lehtsaar E, Vaupel A (2022) Digging deeper: microbial communities in subsoil are strongly promoted by trees in temperate agroforestry systems. Plant Soil 480:423–437

Bi B, Wang Y, Wang K, Zhang H, Fei H, Pan R, Han F (2022) Changes in microbial metabolic C- and N- limitations in the rhizosphere and bulk soils along afforestation chronosequence in desertified ecosystems. J Environ Manage 303:114215

Bilyera N, Kuzyakova I, Guber A, Razavi BS, Kuzyakov Y (2020) How "hot" are hotspots: Statistically localizing the high-activity areas on soil and rhizosphere images. Rhizosphere 16:100259

Blagodatskaya E, Blagodatsky S, Anderson TH, Kuzyakov Y (2009) Contrasting effects of glucose, living roots and maize straw on microbial growth kinetics and substrate availability in soil. Eur J Soil Sci 60:186–197

Bligh EG, Dyer WJ (1959) A rapid method of total lipid extraction and purification. Can J Biochem Physiol 37:911–917

Brandt L, Stache F, Poll C, Bramble DS, Schöning I, Schrumpf M, Ulrich S, Kaiser K, Mikutta R, Mikutta C, Oelmann C, Konrad A, Siemens J, Kandeler E (2023) Mineral type and land-use intensity control composition and functions of microorganisms colonizing pristine minerals in grassland soils. Soil Biol Biochem 182:109037

Cai G, Vanderborght J, Klotzsche A, Van Der Kruk J, Neumann J, Hermes N, Vereecken H (2016) Construction of minirhizotron facilities for investigating root zone processes. Vadose Zone Journal 15:1–13

Chen L, Liu L, Qin S, Yang G, Fang K, Zhu B, Kuzyakov Y, Chen P, Xu Y, Yang Y (2019) Regulation of priming effect by soil organic matter stability over a broad geographic scale. Nat Commun 10:5112

Dennis PG, Miller AJ, Hirsch PR (2010) Are root exudates more important than other sources of rhizodeposits in structuring rhizosphere bacterial communities? FEMS Microbiol Ecol 72:313–327

Dick RP, Kandeler E (2005) Enzymes in soils. In: Hillel D (ed) Encyclopedia of soils in the environment. Elsevier, Oxford, pp 448–456

Driouich A, Follet-Gueye ML, Gibouin MV, Hawes M (2013) Root border cells and secretions as critical elements in plant host defense. Curr Opin Plant Biol 16:489–495

Eichlerová I, Homolka L, Žifčáková L, Lisá L, Dobiášová P, Baldrian P (2015) Enzymatic systems involved in decomposition reflects the ecology and taxonomy of saprotrophic fungi. Fungal Ecol 13:10–22

Federle TW (1986) Microbial distribution in soil-new techniques. In: Megusar F, Gantar M (eds) Perspectives in microbial ecology. Slovene Society for Microbiology, Ljubljana, pp 493–498

Ferraz de Almeida R, Naves ER, Pinheiro da Mota R (2015) Soil quality: Enzymatic activity of soil β-glucosidase. Global Journal of Agricultural Research and Reviews 3:146–150

Fierer N, Schimel JP, Holden PA (2003) Variations in microbial community composition through two soil depth profiles. Soil Biol Biochem 35:167–176

Fox J, Weisberg S (2019) An R companion to applied regression, Third edition. Sage, Thousand Oaks CA. https://socialsciences.mcmaster.ca/jfox/Books/Companion/

Frostegård Å, Tunlid A, Bååth E (1991) Microbial biomass measured as total lipid phosphate in soils of different organic content. Journal of Microbial Methods 14:151–163

Galindo-Castañeda T, Lynch JP, Six J, Hartmann M (2022) Improving soil resource uptake by plants through capitalizing on synergies between root architecture and anatomy and root-associated microorganisms. Front Plant Sci 13:827369

Galindo-Castañeda T, Hartmann M, Lynch JP (2023) Location: root architecture structures rhizosphere microbial associations. J Exp Bot 75:595–604

Gianfreda L (2015) Enzymes of importance to rhizosphere processes. Journal of Soil Science and Plant Nutritions 15(2):283–306

Gobran GR, Clegg S (1996) A conceptual model for nutrient availability in the mineral soil-root system. Can J Soil Sci 76:125–131

Guber A, Blagodatskaya E, Juyal A, Razavi BS, Kuzyakov Y, Kravchenko A (2021) Time-lapse approach to correct

deficiencies of 2D soil zymography. Soil Biol Biochem 157:108225
Habib-ur-Rahman M, Ahmad A, Raza A, Hasnain MU, Alharby HF, Alzahrani YM, Bamagoos AA, Hakeem KR, Ahmad S, Nasim W (2022) Impact of climate change on agricultural production; issues, challenges, and opportunities in Asia. Front Plant Sci 13:925548
Han J, Xia D, Li L, Sun L, Yang K, Zhang L (2009) Diversity of culturable bacteria isolated from root domains of moso bamboo (Phyllostachys edulis). Microb Ecol 58:363–373
Hao C, Dungait JAJ, Wie X, Ge T, Kuzyakov Y, Cui Z, Tian J, Zhang F (2022) Maize root exudate composition alters rhizosphere bacterial community to control hotspots of hydrolase activity in response to nitrogen supply. Soil Biol Biochem 170:108717
Heitkötter J, Marschner B (2018) Is there anybody out there? Substrate availability controls microbial activity outside of hotspots in subsoils. Soil Systems 2:35
Högberg P, Högberg MN, Göttlicher SG, Betson NR, Keel SG, Metcalfe DB, Campbell C, Schindlbacher A, Hurry V, Lundmark T, Linder S, Näsholm T (2007) High temporal resolution tracing of photosynthate carbon from the tree canopy to forest soil microorganisms. New Phytol 177:220–228
Iannucci A, Canfora L, Nigro F, De Vita P, Beleggia R (2021) Relationships between root morphology, root exudate compounds and rhizosphere microbial community in durum wheat. Appl Soil Ecol 158:103781
Inamdar A, Sangawe V, Adhapure N (2022) Enzymes in rhizosphere engineering. In: Dubey RC, Kumar P (eds) Rhizosphere Engineering. Academic Press, Boca Raton, pp 259–272
Jacoby R, Peukert M, Succurro A, Koprivova A, Kopriva S (2017) The role of soil microorganisms in plant mineral nutrition-current knowledge and future directions. Front Plant Sci 8:1617
Joergensen RG (1996) The fumigation-extraction method to estimate soil microbial biomass: calibration of the KEC value. Soil Biol Biochem 28:25–31
Joergensen RG, Wichern F (2018) Alive and kicking: Why dormant soil microorganisms matter. Soil Biol Biochem 116:419–430
Kandeler E (2015) Physiological and biochemical methods for studying soil biota and their functions. In: Paul EA (ed) Soil Microbiology, Ecology and Biochemistry, 4th edn. Academic Press, San Diego, pp 187–222
Kang Y, Rambla C, Haeften SV, Fu B, Akinlade O, Potgieter AB, Borrell AK, Mace E, Jordan DR, Alahmad S, Hickey LT (2024) Seminal root angle is associated with root system architecture in durum wheat. Food and Energy Security 13:e570
Kennedy AC, de Luna LZ (2005) Rhizosphere. In: Hillel D (ed) Encyclopedia of soils in the environment. Elsevier, Oxford, pp 399–406
Konkol NR, McNamara CJ, Hellmann E, Mitchell R (2012) Early detection of fungal biomass on library materials. J Cult Herit 13:115–119
Kramer C, Gleixner G (2008) Soil organic matter in soil depth profiles: Distinct carbon preferences of microbial groups during carbon transformation. Soil Biol Biochem 40:425–433
Kramer S, Marhan S, Haslwimmer H, Ruess L, Kandeler E (2013) Temporal variation in surface and subsoil abundance and function of the soil microbial community in an arable soil. Soil Biol Biochem 61:76–85
Kuzyakov Y, Blagodatskaya E (2015) Microbial hotspots and hot moments in soil: Concept & review. Soil Biol Biochem 83:184–199
Kuzyakov Y, Xu X (2013) Competition between roots and microorganisms for nitrogen: mechanisms and ecological relevance. New Phytol 198:656–669
Langridge P, Braun H, Hulke B, Ober E, Prasanna BM (2021) Breeding crops for climate resilience. Theor Appl Genet 134:1607–1611
Leckie SE, Prescott CE, Grayston SJ, Neufeld JD, Mohn WW (2004) Comparison of chloroform fumigation-extraction, phospholipid fatty acid, and DNA methods to determine microbial biomass in forest humus. Soil Biol Biochem 3:529–532
Liu X, Burslem DFRP, Taylor JD, Taylor AFS, Khoo E, Majalap-Lee N, Helgason T, Johnson D (2018) Partitioning of soil phosphorus among arbuscular and ectomycorrhizal trees in tropical and subtropical forests. Ecol Lett 21:713–723
Lynch JP (2011) Root phenes for enhanced soil exploration and phosphorus acquisition: tools for future crops. Plant Physiol 156:1041–1049
Lynch JP (2013) Steep, cheap and deep: an ideotype to optimize water and N acquisition by maize root systems. Ann Bot 112:347–357
Lynch JP (2019) Root phenotypes for improved nutrient capture: an underexploited opportunity for global agriculture. New Phytol 223:548–564
Lynch JP (2022) Harnessing root architecture to address global challenges. Plant J 109:415–431
Ma X, Razavi BS, Holz M, Blagodatskaya E, Kuzyakov Y (2017) Warming increases hotspot areas of enzyme activity and shortens the duration of hot moments in the root-detritusphere. Soil Biol Biochem 107:226–233
Ma X, Zarebanadkouki M, Kuzyakov Y, Blagodatskaya E, Pausch J, Razavi BS (2018) Spatial patterns of enzyme activities in the rhizosphere: Effects of root hairs and root radius. Soil Biol Biochem 118:69–78
Maillard F, Didion M, Fauchery L, Bach C, Buée M (2018) N-Acetylglucosaminidase activity, a functional trait of chitin degradation, is regulated differentially within two orders of ectomycorrhizal fungi: Boletales and agaricales. Mycorrhiza 28:391–397
Makoi JHJR, Ndakidemi PA (2008) Selected soil enzymes: Examples of their potential roles in the ecosystem. Afr J Biotech 7:181–191
Manschadi AM, Christopher JT, DeVoil P, Hammer GL (2006) The role of root architectural traits in adaptation of wheat to water-limited environments. Funct Plant Biol 33:823–837
Martre P, Quilot-Turion B, Luquet D, Memmah MMOS, Chenu K, Debaeke P (2015) Chapter 14 – Model-assisted phenotyping and ideotype design. In: Sadras VO, Calderini DF (eds) Crop physiology: Applications for genetic improvement and agronomy. Academic Press, San Diego, pp 349–373

Marx MC, Wood M, Jarvis SC (2001) A microplate fluorimetric assay for the study of enzyme diversity in soils. Soil Biol Biochem 33:1633–1640

Mijangos I, Becerril JM, Albizu I, Epelde L, Garbisu C (2009) Effects of glyphosate on rhizosphere soil microbial communities under two different plant compositions by cultivation-dependent and -independent methodologies. Soil Biol Biochem 41:505–513

Moorhead DL, Rinkes ZL, Sinsabaugh RL, Weintraub MN (2013) Dynamic relationships between microbial biomass, respiration, inorganic nutrients and enzyme activities: informing enzyme-based decomposition models. Front Microbiol 4:223

Moorhead DL, Sinsabaugh RL, Hill BH, Weintraub MN (2016) Vector analysis of ecoenzyme activities reveal constraints on coupled C, N and P dynamics. Soil Biol Biochem 93:1–7

Nakhforoosh A, Nagel KA, Fiorani F, Bodner G (2019) Deep soil exploration vs. topsoil exploitation: distinctive rooting strategies between wheat landraces and wild relatives. Plant Soil 459:397–421

Olsson PA, Francis R, Read DJ, Söderström B (1998) Growth of arbuscular mycorrhizal mycelium in calcareous dune sand and its interaction with other soil micro-organisms as estimated by measurement of specific fatty acids. Plant Soil 201:9–16

Paez-Garcia A, Motes CM, Scheible WR, Chen R, Blancaflor EB, Monteros MJ (2015) Root traits and phenotyping strategies for plant improvement. Plants 4:334–355

Pinheiro JC, Bates DM (2000) Mixed-effects models in S and S-PLUS. Springer, New York. https://doi.org/10.1007/b98882

Poll C, Ingwersen J, Stemmer JM, Gerzabek MH, Kandeler E (2006) Mechanisms of solute transport affect small-scale abundance and function of soil microorganisms in the detritusphere. Eur J Soil Sci 57:583–595

R Core Team (2020) R: A language and environment for statistical computing. R foundation for statistical computing, Vienna. URL: https://www.R-project.org/

Rambla C, Van Der Meer S, Voss-Fels KP, Makhoul M, Obermeier C, Snowdon R, Ober ES, Watt M, Alahmad S, Hickey LT (2022) A toolkit to rapidly modify root systems through single plant selection. Plant Methods 18:1–13

Ravi RK, Muthukumar T (2024) Root exudates and their importance in arbuscular mycorrhizal symbiosis and nutrients navigation from inaccessible soil: An efficient mediator of mineral acquisition in nutrient deprived soil. In: Ansari RA, Rizivi R, Mahmood I (eds) Mycorrhizal symbiosis and agroecosystem restoration. Springer, Singapore, pp 101–123

Razavi BS, Zarebanadkouki M, Blagodatskaya E, Kuzyakov Y (2016) Rhizosphere shape of lentil and maize: spatial distribution of enzyme activities. Soil Biol Biochem 96:229–237

Razavi BS, Zhang X, Bilyera N, Guber A, Zarebanadkouki M (2019) Soil zymography: Simple and reliable? Review of current knowledge and optimization of the method. Rhizosphere 11:100161

Ropitaux M, Bernard S, Follet-Gueye ML, Vicré M, Boulogne I, Driouich A (2019) Xyloglucan and cellulose form molecular cross-bridges connecting root border cells in pea (Pisum sativum). Plant Physiol Biochem 139:191–196

Sanaullah M, Razavi BS, Blagodatskaya E, Kuzyakov Y (2016) Spatial distribution and catalytic mechanisms of β-glucosidase activity at the root-soil interface. Biol Fertil Soils 52:505–514

Sasse J, Martinoia E, Northen T (2018) Feed your friends: Do plant exudates shape the root microbiome? Trends Plant Sci 23:25–41

Shang W, Razavi BS, Yao S, Hao C, Kuzyakov Y, Blagodatskaya E, Tian J (2023) Contrasting mechanisms of nutrient mobilization in rhizosphere hotspots driven by straw and biochar amendment. Soil Biol Biochem 187:109212

Smalla K, Wieland G, Buchner A, Zock A, Parzy J, Kaiser S, Roskot N, Heuer H, Berg G (2001) Bulk and rhizosphere soil bacterial communities studied by denaturing gradient gel electrophoresis: plant-dependent enrichment and seasonal shifts revealed. Appl Environ Microbiol 67:4742–4751

Spohn M, Kuzyakov Y (2014) Spatial and temporal dynamics of hotspots of enzyme activity in soil as affected by living and dead roots—a soil zymography analysis. Plant Soil 379:67–77

Spohn M, Carminati A, Kuzyakov Y (2013) Soil zymography a novel in situ method for mapping distribution of enzyme activity in soil. Soil Biol Biochem 58:275–280

Steidinger BS, Turner BL, Corrales A, Dalling JW (2015) Variability in potential to exploit different soil organic phosphorus compounds among tropical montane tree species. Funct Ecol 29:121–130

Steinauer K, Chatzinotas A, Eisenhauer N (2016) Root exudate cocktails: the link between plant diversity and soil microorganisms? Ecol Evol 6:7387–7396

Tabatabai MA (1994) Soil enzymes. In: Weaver RW, Angle SJ, Bottomley PJ, Bezdicek D, Smith S, Tabatabai T, Wollum, A (eds) Methods of soil analysis. Part 2. Microbiological and biochemical properties. Soil Science Society of America, Madison, pp 835–864

Ulrich DEM, Clendinen CS, Alongi F, Mueller RC, Chu RK, Toyoda J, Gallegos-Graves LV, Goemann HM, Peyton B, Sevanto S, Dunbar J (2022) Root exudate composition reflects drought severity gradient in blue grama (*Bouteloua gracilis*). Sci Rep 12:12581

Van der Bom FJT, Williams A, Bell MJ (2020) Root architecture for improved resource capture: trade-offs in complex environments. J Exp Bot 71:5752–5763

Vance ED, Brookes PC, Jenkinson DS (1987) An extraction method for measuring soil microbial biomass C. Soil Biol Biochem 19:703–707

Venzke Filho SP, Feigl BJ, Piccolo MC, Fante L Jr, Siqueira Neto M, Cerri CC (2004) Root systems and soil microbial biomass under no-tillage system. Scientia Agricola 61:529–537

Voss-Fels KP, Snowdon RJ, Hickey LT (2018) Designer roots for future crops. Trends Plant Sci 23:957–960

Wang Q, Wang Y, Wang S, He T, Liu L (2014) Fresh carbon and nitrogen inputs alter organic carbon mineralization and microbial community in forest deep soil layers. Soil Biol Biochem 72:145–151

Weihermüller L, Huisman JA, Lambot S, Herbst M, Vereecken H (2007) Mapping the spatial variation of soil water content at the field scale with different ground penetrating radar techniques. J Hydrol 340:205–216